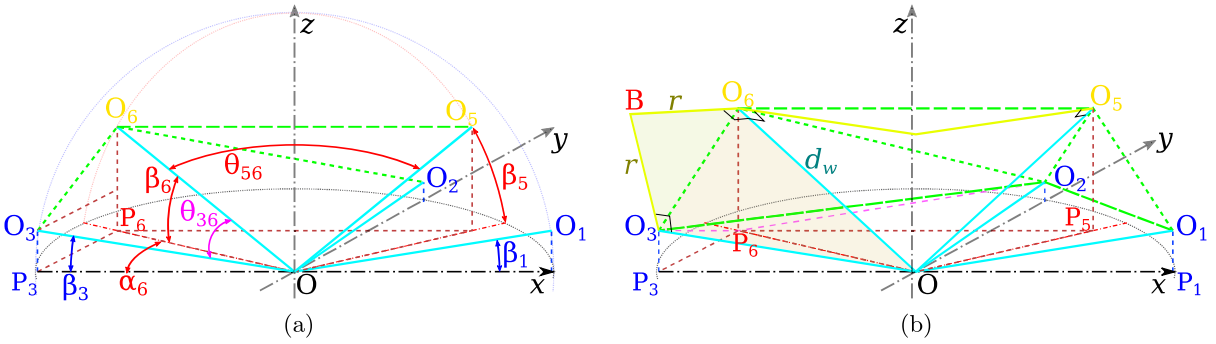

Figure IV.7: Representation of (a) the angles and (b) lengths definitions.

one can see, each angle θ_{ij} is defined as:

$$\theta_{ij} = 2\arcsin\left(\frac{d_{ij}}{2d_w}\right) \tag{IV.1}$$

with the length $d_{ij} = O_iO_j = \sqrt{P_iP_j^2 + (O_jP_j - O_iP_i)^2}$, where

$$P_iP_j = \sqrt{OP_i^2 + OP_j^2 - 2(OP_i)(OP_j)\cos\alpha_j} \quad (\text{here } \alpha_j = 45°) \tag{IV.2}$$

$$O_iP_i = d_w \sin\beta_i \tag{IV.3}$$

$$O_jP_j = d_w \sin\beta_j \tag{IV.4}$$

$$OP_i = d_w \cos\beta_i \tag{IV.5}$$

$$OP_j = d_w \cos\beta_j \tag{IV.6}$$

Similarly, the angle between two adjacent mobile coils j_1 and j_2 is derived as:

$$\theta_{j_1j_2} = 2\arcsin\left(\frac{d_{j_1j_2}}{2d_w}\right) \tag{IV.7}$$

where $d_{j_1j_2} = O_{j_1}O_{j_2} = \sqrt{OP_{j_1}^2 + OP_{j_2}^2}$. If all mobile coils j have the same moving angle β_j, then we obtain: $d_{j_1j_2} = \sqrt{2}d_w\cos\beta_j$ from (IV.6).

When a stationary coil i touches a mobile coil j, their radii must be:

$$r_{ij} = \frac{d_{ij}}{2\cos(\theta_{ij}/2)} = \frac{d_{ij}}{2\sqrt{1 - \left(\frac{d_{ij}}{2d_w}\right)^2}} \tag{IV.8}$$

and when a mobile coil j_1 is in contact with a mobile coil j_2, their radii are defined as:

$$r_{j_1j_2} = \frac{d_{j_1j_2}}{2\cos(\theta_{j_1j_2}/2)} = \frac{d_{j_1j_2}}{2\sqrt{1 - \left(\frac{d_{j_1j_2}}{2d_w}\right)^2}} \tag{IV.9}$$

Since all radii are equal, we get: $r_{\max} = r_{ij} = r_{j_1j_2}$. Hence, it can be shown that the maximal admissible radii are obtained when

$$2 - \sqrt{2}\cos(\beta_i)\cos(\beta_j) - 2\sin(\beta_i)\sin(\beta_j) = 2\cos(\beta_j)^2 \tag{IV.10}$$

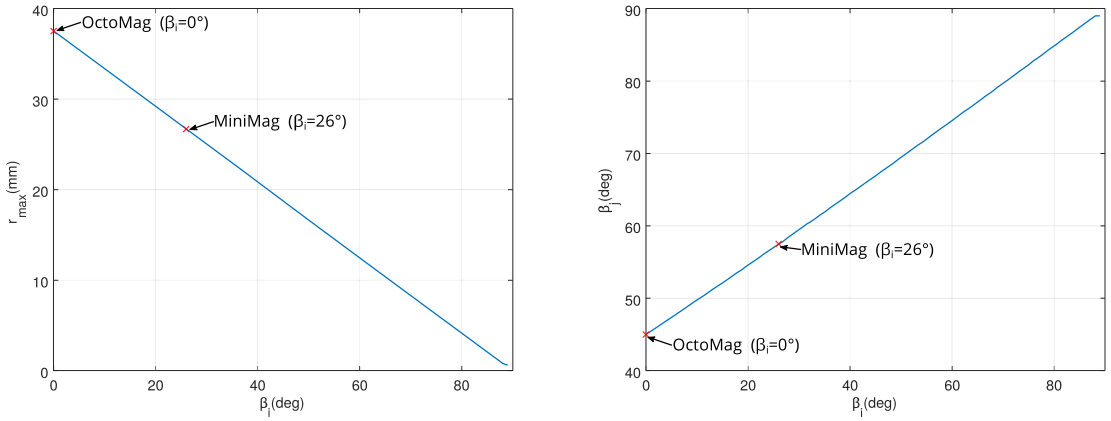

(a) (b)

Figure IV.8: Evolution of (a) admissible radius $r_{\max}$ and (b) the mobile angle β_j when the contact constraints are satisfied.

Figure IV.8 shows the evolution of the admissible radius $r_{\max}$ and of mobile angle β_j when the contact constraints are satisfied. For instance, when the OctoMag configuration is considered, $\beta_i = 0$ for the stationary coil set leads to $\beta_j = 45°$ for the moving coil set (or the upper set equivalently). Obviously, $d_{ij} = d_{j_1 j_2} = d_w$ can be computed from the above equations that brings the maximum coil dimension. Thus, when the d_w is set to $65mm$, the radius of $r_{\max} = 37.5278$ mm can be derived.

IV.2.1.3 Coil implementation

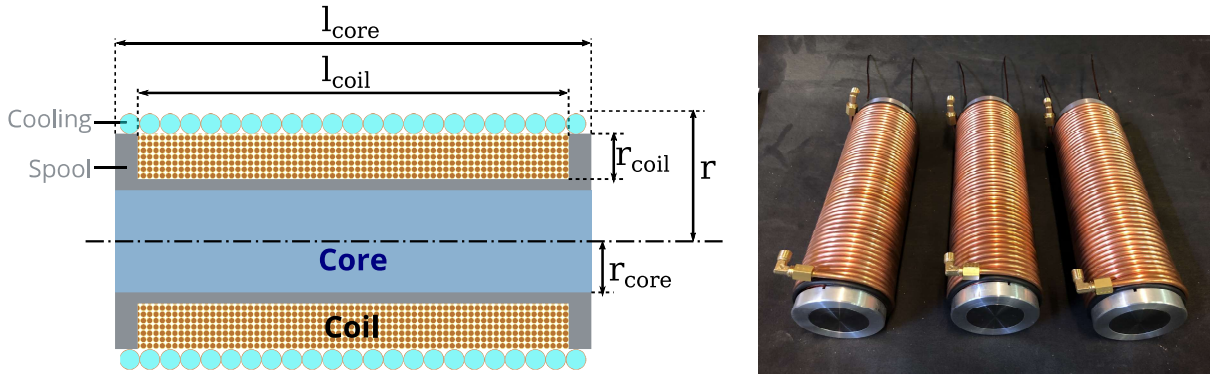

(a) (b)

Figure IV.9: (a) illustrates the electromagnet shape, with its core, coil winding and its cooling part. The spool part allows containing the winding and to separate it from the core. (b) presents the implemented electromagnet prototype.

As specified, a cylindrical electromagnetic coil depicted in figure IV.9a is considered in this study. In such case, the magnetic performance can be approximated using the solenoid model. Indeed, the magnetic field strength at the ends of a infinite solenoid corresponding to an

electromagnet e is given by [148] through applying the Ampère's law (II.1):

$$\|\mathbf{B}_e\| = \mu \frac{i_e N}{2l} \tag{IV.11}$$

with i_e the electric current, l the length of the solenoid, and N the number of turns of the coil winding.

To maximize the magnetic field strength, two parts of the electromagnet can be optimized: i) the core and its permeability performance μ; and ii) the coil winding. To do so, when the maximum allowable electromagnet size $r_{\max}$ with respect to the spatial arrangement is obtained, its remaining dimensions could be determined easily. Kummer [147] has proposed a electromagnet design that takes into consideration further constraints. Specifically, they have shown that the proper length to radius ratio of the core should be at least $l_{core}/r_{core} \geq 8$ to fit properly the above solenoid characteristics. From their results, it appears that a core with a radius of about $r_{core} \approx 20\,\text{mm}$ and then a length $l_{core} = 10 r_{core}$ enable reliable magnetic field performance.

Next, the coil thickness should be determined. From the infinite solenoid (IV.11), the best magnetic performance is achieved when the number of turns N is maximized. However, the winding of coil is limited by the current density that would cause safety problem. Basically, from transformer design, without cooling, it is shown that the current density should not exceed $\mathbf{J}_{\max} = 3\,\text{A/mm}^2$. Nevertheless, to enable strong magnetic field, the current i_e must be high enough. Therefore, the parameter of $\mathbf{J}_{\max} = 3\,\text{A/mm}^2$ normally requires the wire made of a larger cross-section of conductor that will thus limit the number of turns N. In order to increase i_e together with a great N in a limited room, a cooling system will be mandatory. Different strategies can be envisioned for the cooling part, such as using fan, radiator vent, or water/coolant system. Classically, using a circulating coolant is the most effective technology to cool a system.

From these considerations, we have chosen the following design parameters to implement each electromagnet. The core is composed of low carbon steel (C35, ThyssenKrupp AG, France) with $r_{core} = 21\,\text{mm}$ and $l_{core} = 240\,\text{mm}$. An aluminum[8] (Aluminum EN AW-2017a-en 573-3, ThyssenKrupp AG, France) spool is added to separate the core and the coil, and to keep the winding in the given space. This spool has an inner length of $l_{coil} = 210\,\text{mm}$ and a thickness of 1 mm. The coil is composed of winding of 6 layers of copper[9] wire (Enameled copper wire, cl 200 degrees, diameter 1.60mm, grade 2. APX, France) of size of 1.6 mm, leading to a thickness of 9.6 mm and a number of turns $N = 787$. Finally, a cooling unit is built around the coil winding. The cooling system consists of a circulating coolant liquid flowing through a copper tube with a diameter of 4 mm. All these elements lead to an electromagnet with a overall size of $r = 35.6\,\text{mm}$, and electromagnet prototype has been realized shown in figure IV.9b.

IV.2.1.4 Coil performance evaluation

The methodology used in the thesis is based on the assumption that the point-dipole model given by Eq. (III.1) approximate properly the magnetic field distribution. The assumption is validated in this section.

FEM modeling using ANSYS® Maxwell[10] software has been performed. Hence, the specified electromagnetic coils have been modeled and simulated through finite element analysis (Finite Element Analysis (FEA)). Figure IV.10 shows some simulation results where a current of 1 A/turn

[8] Aluminum is a paramagnetic material that is essentially unaffected by the magnetic fields.

[9] Copper is a diamagnetic material, and thus is repelled by the magnetic field.

[10] `https://www.ansys.com/products/electronics/ansys-maxwell`